www.ptcer.pl/mccm

MATERIAŁY CERAMICZNE /CERAMIC MATERIALS/, 69, 4, (2017), 380-387

Porosity evolution during sintering in cold isostatically and filter pressed compacts of nanozirconia powders

Waldemar Pyda

AGH University of Science and Technology, Faculty of Materials Science and Ceramics,
al. A. Mickiewicza 30, 30-059 Kraków, Poland
e-mail: pyda@agh.edu.pl

Abstract

The nanopowders 3 mol% Y_2O_3-ZrO_2 with different size of crystallites and degree of agglomeration were tested. Two nanopowders were obtained by a co-precipitation technique together with the controlled crystallization of the resulting sediment under hydrothermal and calcination conditions. They had a crystallite size of 8 nm and 20 nm (D_{111t}), respectively, and showed a respective modal particle size (D_{50}) of 7.3 nm and 1640 nm. The third submicron powder (D_{111t} = 25 nm, D_{50} = 1700 nm) was of commercial origin. The nanopowders were formed by isostatic and filtration pressing, and then pressureless-sintered in the air. The basic properties of powders were characterized, and their behaviour during heat treatment was investigated in the range from room temperature to 1600°C. Changes in phase composition, porosity, pore size and relative density as a function of temperature were determined. A significant effect of the morphology of the nanopowders on the beginning and maximum temperatures of the shrinkage of the samples as well as on the temperature at which open pores closed was found. A transient increase in the size of open pores in the sintered samples was observed, depending on the initial morphology of the nanopowders. The temperature of the beginning of the growth of the pore size and its scale was dependent on the initial pore size in the compacts, which was controlled by the crystallite size of the powder and its agglomeration state. The energy of activation of the processes responsible for the sintering shrinkage of the studied nanopowders was estimated.

Keywords: Porosity evolution, Pore growth, Nano-zirconia, Filter pressing, Sintering

EWOLUCJA POROWATOŚCI PODCZAS SPIEKANIA WYPRASEK NANOPROSZKÓW DWUTLENKU CYRKONU PRASOWANYCH IZOSTATYCZNIE I FILTRACYJNIE

Badaniom poddano nanoproszki 3% mol. Y_2O_3-ZrO_2 o zróżnicowanym rozmiarze krystalitów i stopniu zaglomerowania. Dwa nanoproszki, mające rozmiar krystalitów 8 nm i 20 nm (D_{111t}) przy jednoczesnym modalnym rozmiarze cząstki (D_{50}) odpowiednio 7,3 nm i 1640 nm, otrzymano techniką współstrącania wraz z kontrolowaną krystalizacją otrzymanego osadu odpowiednio w warunkach hydrotermalnych i prażenia. Trzeci submikronowy proszek (D_{111t} = 25 nm, D_{50} = 1700 nm) był pochodzenia handlowego. Nanoproszki formowano drogą prasowania izostatycznego i filtracyjnego, a potem spiekano swobodnie w powietrzu. Scharakteryzowano podstawowe właściwości proszków i zbadano ich zachowanie się podczas obróbki cieplnej w zakresie od temperatury pokojowej do 1600°C. Określono zmiany składu fazowego, porowatości, wielkości porów i gęstości względnej w funkcji temperatury. Stwierdzono istotny wpływ morfologii nanoproszków na temperatury początku i maksimum skurczu próbek, a także na temperaturę, w której wystąpiło zamykanie się porów otwartych. Zaobserwowano przejściowy wzrost rozmiaru porów otwartych w spiekających się próbkach zależny od wyjściowej morfologii nanoproszków. Temperatura początku wzrostu rozmiaru porów oraz jego skala zależne były od wyjściowego rozmiaru porów w wypraskach, który kontrolowany był przez wielkość krystalitów proszku i stan jego zaglomerowania. Oszacowano energię aktywacji procesów odpowiedzialnych za skurcz spiekania badanych nanoproszków.

Słowa kluczowe: ewolucja porowatości, rozrost porów, nanometryczny tlenek cyrkonu, prasowanie filtracyjne, spiekanie

1. Introduction

The continuing interest in the properties of nanocrystalline solids induces the need to develop reliable technologies for their production in the form of products with unlimited sizes and shapes. The processing of nanocrystalline powders with the techniques typical of the technology of obtaining dense polycrystalline ceramics, consisting of molding them, e.g. by pressing and sintering the formed raw shapes into nanocrystalline sintered materials, presents many problems. Some of them, especially those related to the issue of grains minimization and simultaneous maximization of densification of sintered bodies were reviewed by Mayo *et.al.* [1]. The cited work analyzed, among others the issue of sinter density changes as a function of the sintering temperature of morphologically different nanocrystalline and submicron powders. With full awareness of the fact that the densification of polycrystals is extremely sensitive to microstructural features, such as the size of the pores, the changes in the porosity of the sintered materials during their heating are not shown.

ISSN 1505-1269

In connection with the above, the aim of the presented work is to characterize the influence of morphological features of powders, especially in relation to the size of crystallites/particles in the nano and submicron range on the evolution of porosity and densification during heat treatment of zirconia powders. The work uses isostatic and filtration compaction for initial densification of powders into raw shapes as well as heat treatment under pressureless sintering as a method of their consolidation.

2. Experimental part

Two nanocrystalline zirconium dioxide powders containing 3 mol% Y_2O_3 in a solid solution were prepared by the method of co-precipitation of a homogeneous sediment of both hydrated zirconia and its crystallization under the conditions of hydrothermal treatment (NZ8) and calcination (NZ20). The use of different crystallization techniques gave the possibility of obtaining powders not only differing in the size of crystallites, but also the state of agglomeration

A common aqueous solution of yttrium(III) chloride (Y_2O_3 with a purity of 99.99% as a precursor) and zirconium(IV) oxychloride octahydrate ($ZrOCl_2 \cdot 8H_2O$ with purity > 99.5%) or zirconium(IV) chloride ($ZrCl_4$ with purity > 98%) was used in the preparation of the NZ8 and NZ20 nanopowder, respectively. An aqueous solution of ammonia was taken as a precipitation reagent in an amount ensuring pH = 9 of liquid over the co-precipitated sediment. Ammonium chloride, an unnecessary co-precipitation product was removed by rinsing the precipitate with distilled water

The precipitate, the precursor of the NZ8 powder, was subjected to a hydrothermal treatment for 4 hours at 240 °C under the pressure of saturated water vapour at this temperature. The crystalline powder was dried at 120 °C and milled for 1 hour in a mixing mill with grinding media made of 3Y-TZP with a diameter of 2 mm in an isopropyl alcohol environment

The precipitate, the NZ20 powder precursor, was subjected to additional washing with ethyl alcohol until the filtrate had an ethanol concentration of 70% by volume. The precipitate dried to constant mass was calcined for 1 hour at 950 °C. The loss of calcination amounted to 31%. The calcined material was subjected to attrition grinding for 4 hours in a mixing grinder with Y-TZP grinding media with a diameter of 2 mm in an aqueous solution of ammonia 1:10.

In accordance with the stated objective, the study included the submicron powder TZ-3Y from Tosoh Corporation containing 3 mol% Y_2O_3 in solid solution with ZrO_2 (NZ25).

All powders were pre-pressed in a steel mould with a diameter of 14 mm at a pressure of 75 MPa and pressed isostatically at a pressure of 300 MPa. 2 wt.% of a 10% oil-in-water emulsion was introduced into the NZ20 powder, the NZ25 powder was compacted without additives as containing inherent compaction improving additives, while 5 wt.% of the oil-in-water emulsion as a lubricant was added to the NZ8 powder; the compacts were marked NZ20-iso, NZ25-iso and NZ8-iso, respetively

Heat treatment of the compacted samples was carried out at temperatures of 500–1600 °C at a regime of the constant rate of heating (CRH). It consisted in heating samples at a rate of 2 °C/min to a temperature of 500 °C, and then at a rate of 6 °C/min to the selected temperature, and holding it there for 2 minutes. The samples were cooled with the furnace.

The NZ8 powder was used to form slip samples by the filter pressing method. For this purpose, a wet, not heat-dried after hydrothermal treatment, sediment of crystalline powder was used, which contained 51.2% ± 0.2% by weight of water, which is equivalent to the volume fraction of powder particles equal to 13.5%. The sediment was used to prepare the slurry, which contained 9.4 vol.% powder particles and 10.7 wt.% sucrose (per 100 g of dry powder) acting as a dispersing agent and lowering the tendency to crack of shaped bodies. The slurry had a viscosity of 5.200 cP at a shear rate of 10 s^{-1} and a practical lack of hysteresis of the flow curve. Samples with a diameter of ~50 mm were formed in a filter press at a pressure of 15 MPa. The formed samples that were marked as NZ8-filtr were dried at room temperature and heat treated together with cold isostatically pressed samples.

The morphology of the powders was observed under a transmission electron microscope (EM301, Philips). The content of monoclinic phase in powders and compacted materials after heat treatment was determined using the X-ray method (Seifert system XRD) according to Ref. [2].The X-ray line broadening of the peak (111) of the tetragonal phase was the basis for estimating the size of crystallites in powders according to Sherrer's formula. The instrumental broadening was removed by an intermediate function between Cauchy and Gauss functions. The particle size distribution of the primary particles in the powders was determined using a laser particle size analyzer (Fritsch Particle Sizer Analysette 22). The specific surface area of the powders was determined by the BET method by means of a single point method (Sorpty 1750, Carlo Erba Strumentazione). Mercury porosimetry was used to characterize the open porosity in the samples (Porosimeter 2000, Carlo Erba Strumentazione). The density of the samples was measured by hydrostatic weighing in water or using geometric dimensions and sample mass. Sintering kinetics as a function of particle size distribution

Table 1. Specific surface area, S_w, monoclinic phase content, V_j, size of tetragonal phase crystallites, D_{111t}, equivalent diameters, D_{BET}, D_{50}, D_m, (mode, average size from microscopic measuremets) and tapped density, r_n, of zirconia powders used in studies.
Tabela 1. Powierzchnia właściwa, S_w, udział fazy jednoskośnej, V_j, wielkość krystalitów fazy tetragonalnej, D_{111t}, średnice zastępcze, D_{BET}, D_{50}, D_m, (moda; pomiary mikroskopowe) oraz gęstość nasypowa z usadem, ρ_n, proszków dwutlenku cyrkonu użytych w badaniach.

Powder	S_w, [m^2/g]	D_{111t} [nm]	D_{BET} [nm]	D_m [nm]	D_{50} [nm]	V_j [vol.%]	ρ_n [g/cm^3]
NZ8	131.6±0.5	8	8.1	8.3	7.3	4.3	1.11±0.03
NZ20	38.0±0.1	20	26	30	1640	32.1	1.28±0.04
NZ25	16.4±0.4	25	61	170	1700	29.0	1.41±0.03

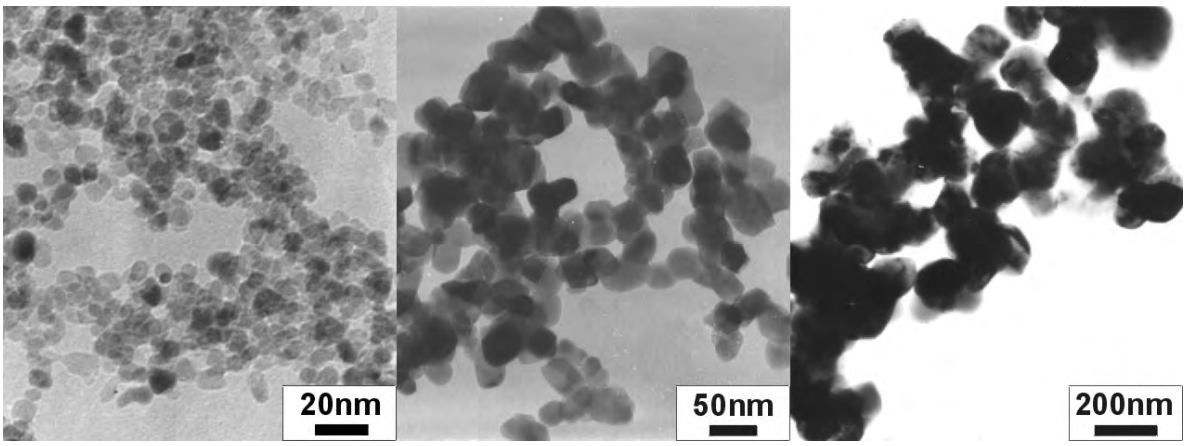

a) b) c)

Fig. 1. Morphology of 3 mol%. Y_2O_3-ZrO_2 powders used for testing: a) NZ8, b) NZ20 and c) NZ25.
Rys. 1. Morfologia proszków 3% mol. Y_2O_3-ZrO_2 użytych do badań: a) NZ8, b) NZ20 i c) NZ25.

Table 2. Densification of starting compacts.
Tabela 2. Zagęszczenie wyjściowych wyprasek.

Sample	Consolidation technique	Apparent density [g/cm^3]	Relative density [%]
NZ25-iso	CIP	3.024±0.012	49.7±0.2
NZ20-iso	CIP	3.057±0.013	50.3±0.3
NZ8-iso	CIP	3.185±0.031	52.4±0.5
NZ8-filtr	Filter pressing	2.870±0.016	47.2±0.9

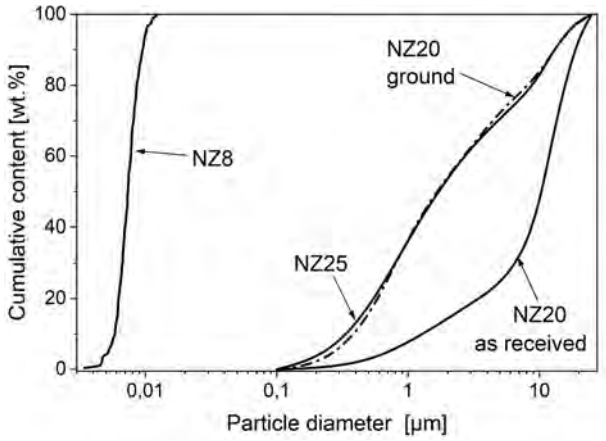

Fig. 2. Particle size distributions of the studied powders.
Rys. 2. Rozkład wielkości ziaren w badanych proszkach.

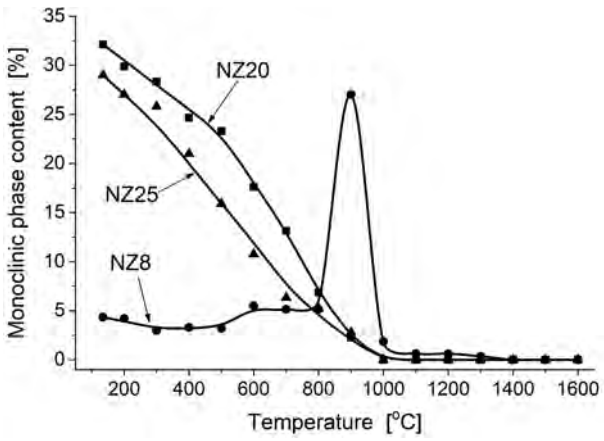

Fig. 3. Changes in the monoclinic phase content involved in heat treatment.
Rys. 3. Zmiany udziału fazy jednoskośnej towarzyszące wygrzewaniu.

was studied during initial sintering by measuring powder compact densification at the applied constant rate of heating, using integral CRH data plots [3].

3. Results and discussion

3.1. Characteristics of powders and green samples

The basic properties of the powders used for the tests are summarized in Table 1, and their morphology is shown in Fig. 1. The powder obtained by the hydrothermal method (NZ8) was characterized by very small (8 nm) crystallite sizes, and thus an extremely large specific surface area of 132 m^2/g. TEM observations reveal the agglomerate structure of this powder (Fig. 1a), and the results of Ref. [4] suggest the presence of weak agglomerates. The calcined powder (NZ20) had higher crystallites (20 nm), and hence, smaller surface area. The agglomerates of NZ20 powder (Fig. 1b) are expected to be stronger when compared to NZ8. The commercial TZ-3Y powder (NZ25) consisted of slightly larger crystallites than NZ20. The specific surface area of NZ20 powder was ~38 m^2/g. NZ20 and NZ25 powders were characterized by a similar monoclinic phase content (Fig. 3). The lowest specific surface area (~16.5 m^2/g) and the largest grain (~100 nm) possessed NZ25 powder (Fig. 1).

The particle size distributions of NZ20 powders before grinding and after grinding are shown in Fig. 2 and indicate a clear reduction in the agglomerate size of the NZ20 powder (from ~15 μm to ~0.8 μm) under the grinding conditions used. It also indicates that a small part of agglomerates has not been ground, as evidenced by the presence of a population of ~15 μm in size. The tapped density measurements (Table 1) show that the TZ-3Y (NZ25) powder, which was in the form of a granulate obtained in a spray dryer, achieved the highest compaction. The remaining powders had lower tapped densities due to the use of a simple but imperfect granulation technique consisting in sieving through a 0.2 mm mesh sieve, and in connection with the resultant non-spherical agglomerate morphology.

Table 2 contains the results of the measurement of apparent and relative densities of the compacts. The physical density of powders was assumed 6.08 g/cm^3 in the relative density calculations. Under the applied consolidation conditions, the hydrothermal powder compact (NZ8-iso) obtained better compaction than the submicron commercial powder one (NZ25-iso), which confirms that nanometric powders characterized by low agglomerate strength can be packed to high densities. The NZ20 powder showed slightly better compactibility than NZ25. The much smaller density of the NZ8-filtr sample than the NZ8-iso one suggests that the filter pressing conditions were not optimal, especially with respect to properties of the slip. Differences in the density of isostatically compressed samples have an undoubted source in the diversified both morphological features of the powders used and mechanical strength of the aggregates or agglomerates of the primary crystallites.

3.2. Characteristics of heat treated samples

The changes in the content of monoclinic phase in the samples tested are shown in Fig. 3. The NZ20 and NZ25 powders showed a common tendency of the monoclinic phase to decrease as the temperature rises. At 1000 °C, the content of monoclinic phase dropped to zero and this state did not change with further increase in temperature. The samples

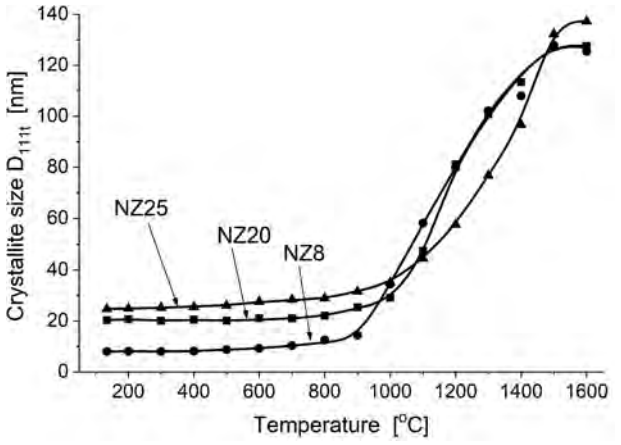

Fig. 4. Crystallite size of the tetragonal phase in compacts obtained from the indicated powders as a function of heat treatment temperature.
Rys. 4. Wielkość krystalitów fazy tetragonalnej w próbkach otrzymanych ze wskazanych proszków w funkcji temperatury obróbki cieplnej.

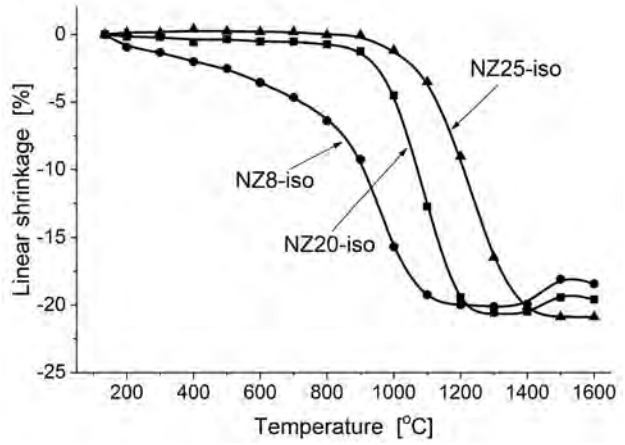

Fig. 5. Linear shrinkage of compacts obtained from the indicated powders as a function of heat treatment temperature.
Rys. 5. Skurcz liniowy wyprasek otrzymanych ze wskazanych proszków w funkcji temperatury obróbki cieplnej.

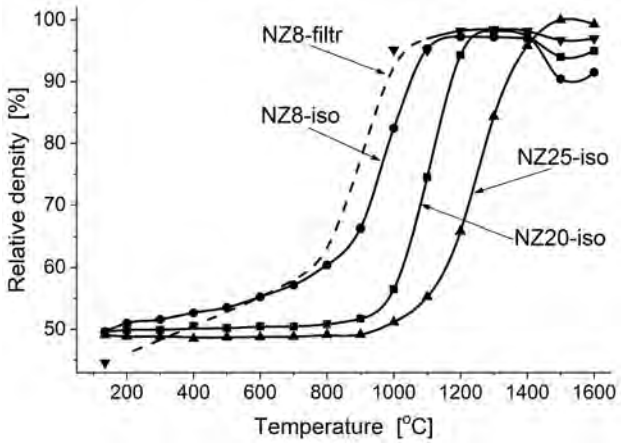

Fig. 6. Relative density as a function of heat treatment temperature. The dashed line is an estimate.
Rys. 6. Gęstość względna w funkcji temperatury obróbki cieplnej. Linia przerywana stanowi oszacowanie.

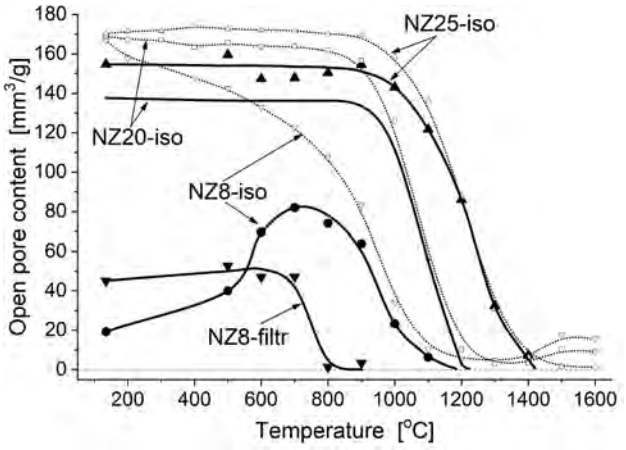

Fig. 7. Open pore content as a function of heat treatment temperature. Corresponding relationships between total porosity and temperature are plotted with dotted lines.
Rys. 7. Udział porów otwartych jako funkcja temperatury obróbki cieplnej. Odpowiednie zależności pomiędzy całkowitą porowatością a temperaturą wykreślone zostały liniami punktowymi.

obtained from the hydrothermally crystallized powder, which were initially poorer in the monoclinic phase than the samples prepared from the calcined powders, show insignificant changes in the phase composition to the temperature of ~500°C, after which a slight increase in the monoclinic phase content was observed, and an extraordinary maximum appeared at ~900 °C. A similar temperature dependence of the phase composition of yttria-zirconia nanopowder of hydrothermal origin was reported by Zych *et al.* [5].

The above reported evolution of the phase composition of the tested zirconia powders in the form of compacts with a different degree of densification is related to the martensitic nature of the t → m transformation, which is diffusionless, accompanied by a negative change in the free-energy chemical driving force, changes in surface/interfacial and elastic strain energies, the need to overcome the nucleation barrier, and usually requires some supercooling [6]. The t → m transformation depends on the size of crystallite (for zirconia powders) and grain (for consolidated zirconia materials) because of the surface and interfacial energy difference, respectively, between the monoclinic and tetragonal polymorph. An additional contribution comes from the elastic strain energy when the transforming grains are embedded in a consolidated tetragonal matrix. An inverse linear relationship between critical crystallite/grain size and transformation temperature has been reported by Suresh and Mayo [7], indicating that the critical t-ZrO_2 size increases with the increase of the transformation temperature. The authors stated that skilful manipulations of the grain size can lower hundreds of degrees the t → m transformation temperature in yttria-stabilized zirconia. It was also evidenced that the zirconia material of a given chemical composition in the solid form has a lower transformation temperature than in the particulate form, when the crystallite and grain sizes are equal. The elastic strain energy involved in the transformation was indicated to be responsible for this difference and for suppression of the t→m transformation to lower temperatures.

The observed increase in the content of monoclinic phase with the maximum of 27.0 wt.% at 900 °C in the case of NZ8 compacts (Fig. 3) is undoubtedly related to exceeding the critical size by tetragonal crystallites, but it seems that this should not be attributed solely to the increase in crystallite size due to the opposite trend shown by the NZ20 and NZ25

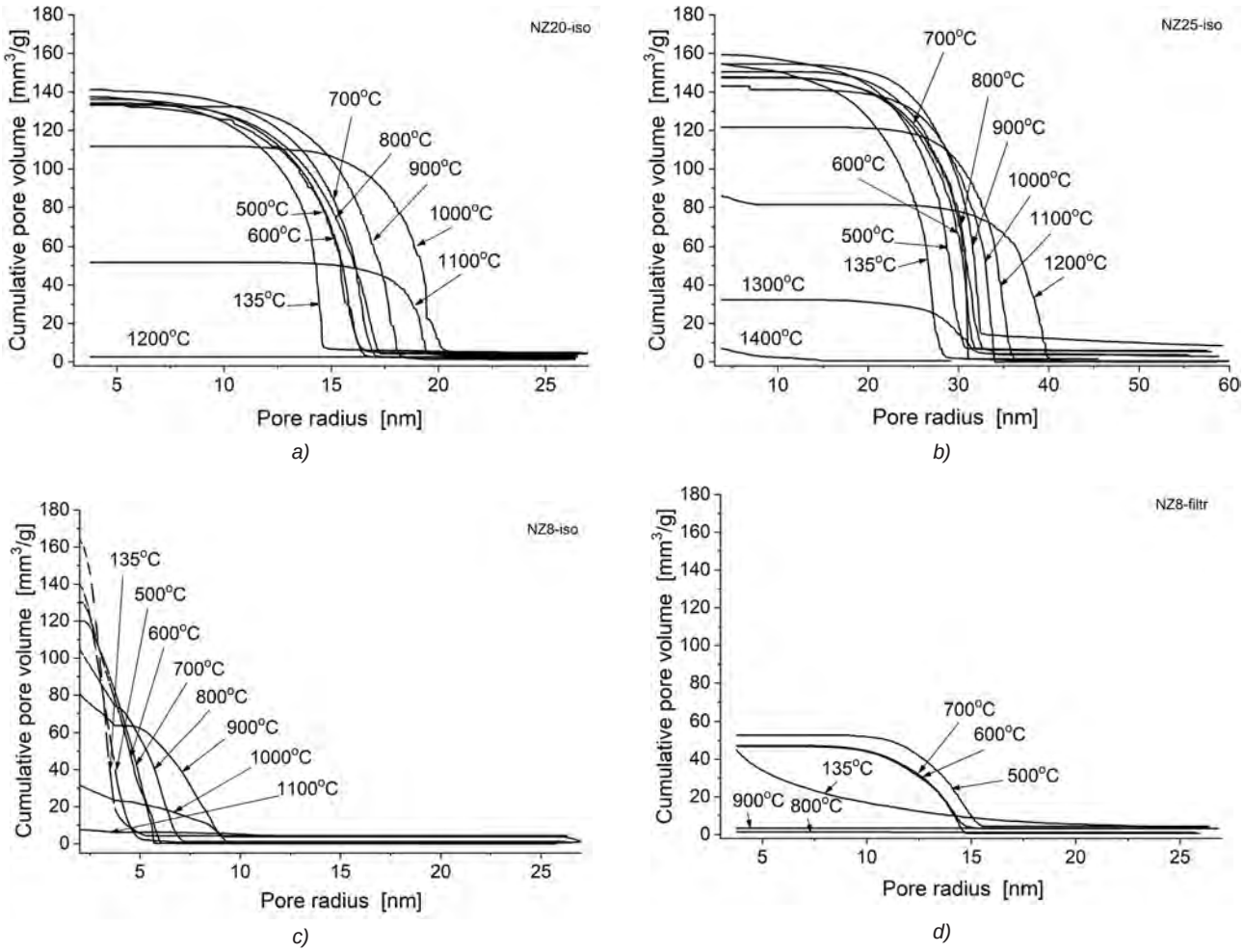

Fig. 8. Cumulative curves of pore size distributions in compacts heated at indicated temperatures: a) NZ20-iso series, b) NZ25-iso series, c) NZ8-iso series (dashed lines are estimates that take into account the total porosity of the samples determined on the basis of their geometrical dimensions and mass), d) NZ8-filtr series.

Rys. 8. Krzywe sumacyjne rozkładów wielkości porów w wypraskach wygrzewanych we wskazanych temperaturach: a) seria NZ20-iso, b) seria NZ25-iso, c) NZ8-iso (liniami przerywanymi wykreślono przebiegi przybliżone uwzględniające porowatość całkowitą próbek określoną na podstawie ich wymiarów geometrycznych i masy), d) seria NZ8-filtr.

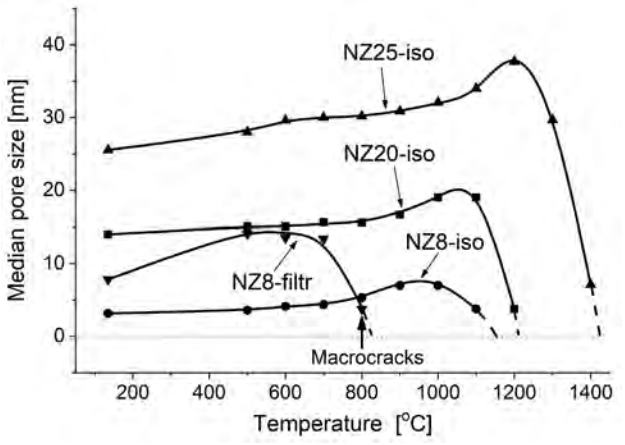

Fig. 9. Median radius of pores in compacts obtained from the indicated powders as a function of heat treatment temperature. Dashed lines are estimates.
Rys. 9. Medialny promień porów w próbkach otrzymanych ze wskazanych proszków jako funkcja temperatury obróbki cieplnej. Linie przerywane stanowią oszacowanie.

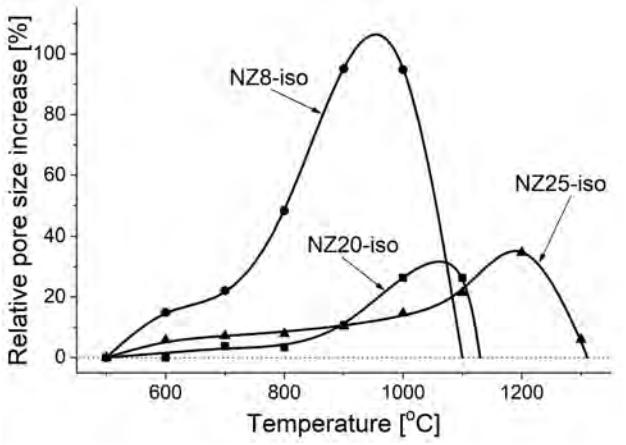

Fig. 10. Dependence of the relative increase in pore size on the temperature and type of powder used.
Rys. 10. Zależność względnego przyrostu rozmiaru porów od temperatury i rodzaju użytego proszku.

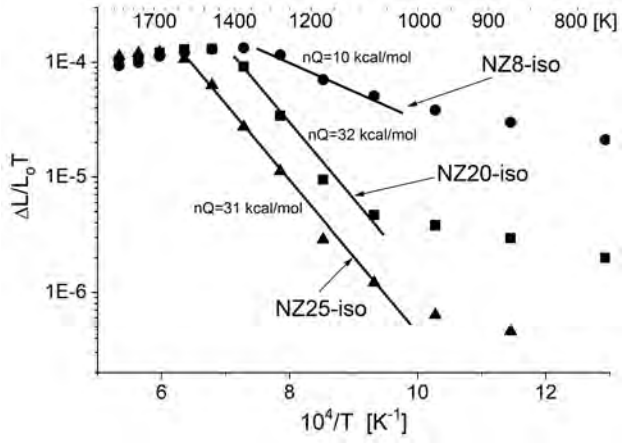

Fig. 11. Linear shrinkage vs. temperature in the Young-Cutler coordinates (CRH method).
Rys. 11. Zależność skurczu od temperatury we współrzędnych zaproponowanych przez Younga-Cutlera dla metody stałej szybkości ogrzewania (CRH method).

compacts. Although the crystallite growth of NZ8 powder shown in Fig. 4 was 80% in the range from room temperature to 900 °C, the crystallite size of 14.5 nm achieved at this temperature was almost or more than twice lower than in the case of NZ20 (25.3 nm) and NZ25 (31.6 nm) calcined powders, respectively, and yet the latter showed at 900 °C a significantly smaller content of monoclinic phase of 2.3 wt.% and 2.8 wt.%, respectively. It should therefore be taken into account that only the NZ8 powder compacts in the considered temperature range showed a significant linear shrinkage of 9.24% (Fig. 5), and an accompanying increase in relative density by 14% to a value of 66.3% (Fig. 6). Under the same conditions, the compacts from the calcined NZ20 and NZ25 powders showed a slight shrinkage of 1.25% and 0.05%, respectively, with a much smaller increase in the crystallite size of 22% and 24%, respectively. The increase in the density of NZ8 compacts is accompanied by the increase in intercrystallite boundaries (proved for analogous zirconia nanopowders by Zych et al. [5] and Lach et al. [10]) at the expense of free surfaces and the change in the shape of grains. Thus, the surface/interfacial energy difference between the monoclinic and tetragonal polymorph changes, and the contribution from the strain energy involved in the transformation becomes important, which, according to the Suresh and Mayo approach [7], should lead to a reduction in the critical size of tetragonal grains. Such reduction in the critical size of tetragonal grains accompanying the increase in the density of NZ8 compacts would explain the observed, transient increase in the monoclinic phase content with temperature.

Progressive enlargement of contacts between crystallites and a change in the shape of crystallites during low-temperature heat treatment of NZ8 compacts can also affect nucleation of the monoclinic phase and lowering the energy of the nucleation barrier. *In-situ* observations by Ma and Rühle [6] demonstrated that heterogeneous nucleation can occur at small-angle grain boundaries, or more frequently at the edges of the grains of tetragonal zirconia polycrystals (TZP). In addition, autocatalytic nucleation could occur in partially sintered NZ8 compacts as in dense TZP materials [6]; the stresses caused by a transforming t-ZrO_2 region are usually transferred to the neighbouring grains, thus causing further nucleation.

Fig. 4 illustrates the change in the size of tetragonal phase crystallites/grains associated with the heating of test samples. Crystallite/grain growth was very limited at temperature rages attributed to the initial state of sintering and dependent on the initial crystallite size; the NZ8 powder composed of 8 nm crystallites showed the highest coarsening rate, and the coarsening commenced at ~500 °C. Greskovitch and Lay suggested the mechanism for coarsening in the early stage of sintering of very porous compacts, being quite different from coalescence and ordinary grain growth [8]. It involves the filling of necks between adjacent grains by surface diffusion or vapour transport followed by the movement of the grain boundary through the smaller grain.

The grain growth rate increases in the intermediate stage of sintering [9]. As shown in Fig. 4, a temperature of significant increase of the grain growth rate, announcing

the beginning of the intermediate sintering stage, was the lower the smaller the initial crystallite size of the powder.

Sintering of powder compacts invariably is accompanied by a shrinkage. The dependence of the shrinkage on the heat treatment temperature shown in Fig. 5 indicates a significant effect of the crystallite size and state of agglomeration of the starting powder on the temperature at which compacts begin to shrink. The NZ8-iso compacts obtained from the hydrothermal nanopowder of the smallest particle size start to shrink at temperatures as low as 200 °C, while the coarse grained calcined powder compacts (NZ20-iso and NZ25--iso) show shrinkage only after exceeding a temperature of 900 °C. The NZ25-iso compacts showed maximum shrinkage at the highest temperature (1500 °C) and were the only ones that showed no expansion at the highest temperatures of heat treatment. The expansion of the NZ8-iso and NZ20--iso compacts was related to atmospheric gas trapped in the pores [9], limiting also the final density (Fig. 6).

Zych *et al.* [5] studied filter pressing of 3 mol% yttria-zirconia hydrothermal nanopowder, and attributed shrinkage of the obtained compacts in the temperature range of 150-300 °C to evaporation of water molecules adsorbed on the powder surface in a layer of 0.2 nm thickness. Lach *et al.* [10] studied sintering behaviour of 8 mol% Y_2O_3-ZrO_2 hydrothermal nanopowder, having the same DTA/TG characteristics as NZ8 nanopowder (not presented) and the nanopowder studied by Zych *et al.* [5]. Mass spectrometric analysis demonstrated the water molecules evolved during heating from the nanopowder at two temperature ranges: 50-200 °C and 300-700 °C with a peak maximum at ~90 °C and ~420 °C, respectively, which corresponded to the maximum of the endothermic peak in the DTA curve. Also in this case, the total shrinkage of nanopowder compacts determined from room temperature to 900 °C was attributed to desorption of the water molecules.

In the case of NZ8 powders and above 700 °C, which is the temperature of complete removal of water molecules from the nanopowder, the sintering rate is clearly increased (Fig. 5), suggesting the effects of the densifying mechanisms related to grain boundary diffusion and lattice diffusion or other.

Changes in the relative density of the tested samples during heat treatment are shown in Fig. 6. An increase in maximum density of sintered bodies is observed, accompanied by an increase in the temperature of the beginning of the intensive density increase. NZ8-iso compacts made of nanocrystalline hydrothermal powder showed an increase in density practically from the lowest heat treatment temperatures, but their final density was lower than that of NZ25-iso compacts, which started to densify only after exceeding the temperature of 900 °C. In contrast to the other samples, the smallest decrease in density at the highest temperatures of heat treatment was observed in the NZ25-iso compacts. Large reduction in the sintering temperature for the nanoscale NZ8 powder is related to the strong particle size dependence of the matter transport rates for the solid state sintering mechanisms. When the densifying mechanisms dominate, then the rate of densification is predicted to vary as $1/G^m$, where G is the particle size, and the exponent m = 4 for grain boundary diffusion and m = 3 for lattice diffusion [9].

Gases trapped in the pores of NZ8 and NZ20 sintered bodies in the final stage of sintering were the reason for their limited final density due to pore coalescence, leading to a phenomenon referred to as bloating [9]. Zhou and Rahaman reported this phenomenon for ultra-fine (10 nm in size) hydrothermal CeO_2 powder [11].

Analysis of the evolution of porosity in compacts shown in Figs. 7–10 sheds some light on the causes of the above described behaviour of the investigated zirconia powders during heat treatment. Fig. 8 shows the cumulative curves of the pore size distributions of the tested compacts determined by mercury porosimetry. The other drawings show relationships between selected characteristic features of these distributions and temperature. Thus Fig. 7 , 9 and 10 illustrates the temperature dependence of open and total pore content, median pore radius, and relative increase in pore size, respectively.

A comparative analysis of the temperature dependence of open pores (Fig. 7), the morphology of the studied powders (Fig. 1) and the temperature dependence of crystallite size (Fig. 4) shows a close relationship between the temperature at which open pores are closed and the crystallite/particle sizes of powder. The most coarse-grained powder of NZ25 gives microstructures in which the pores close at 1400 °C, NZ8-iso compacts obtained from the nano-sized hydrothermal powder had pores closing at temperatures of 300 °C lower. A significant part of the porosity of the NZ8-iso was in the size range unavailable for the mercury porosimeter at the applied maximum pressure (< 4 nm) as evidenced by the course of the corresponding curve of total porosity (Fig. 7) This figure also reveals the fact that for the given powder the temperature at which the pores are closed depends on the applied method of forming which affects particle packing and the resultant pore size distribution. The pores of the NZ8-filtr compact closed at a lower temperature when compared to the NZ8-iso compact.

Graphs of the relationship between the median radius of open pores and temperature shown in Fig. 9 reveal the general regularity of a temporary increase in the pore size when increasing the heat treatment temperature of the compacts. The higher the initial pores in a compact, the higher the temperature needed to trigger the process of reducing their size and the higher the temperature of their closing.

The temperature of the beginning of the pore growth and its extent depend on the pore size, which is directly related to the size of the crystallites/particles of the powder and the forming technique used (compare Figs. 10, 9 and 1). Reducing the size of the pores reduces the temperature of the beginning of the pore growth, and at the same time increases the relative increase in their size during heat treatment.

The following mechanisms can be indicated as responsible for the pore coarsening.

Akash and Mayo [12] presumed that the pore coarsening during initial stage sintering is an indirect consequence of inter-particle neck growth by surface diffusion that leads to surface rounding of pores. For a compact with 62% of theoretical density, they predicted a pore growth factor of 1.28 for pore size increasing, which matches very well with the experimentally observed pore growth factor of 1.27

when zirconia powder with average particle size of 0.3 μm was uniaxially dry pressed at 1.8 GPa and sintered in air at 870 °C. Similar values of pore growth factor were determined for NZ20 and NZ25 powders (Fig. 10).

Exner and Müller [13] have pointed out that the pore coarsening as a consequence of particle rearrangement is an experimental evidence that should be considered in sintering studies. The particle rearrangement is in connection with differential densification [9] due to the formation of small regions with three-dimensional, ordered packing of particles that are separated by voids at the boundaries of the ordered regions. The faster sintering of the ordered regions, when compared to the areas among them, leads to differential stresses that may lead to enlargement of the voids (pores), particle rearrangement or even the generation of crack-like voids in the less dense regions what was the case of NZ8-filtr compacts (Fig. 10). A pore growth factor of ~2 determined for the NZ8-iso compacts should be a consequence of particle rearrangement during differential densification.

It can not be excluded that the zirconia nanocrystallite rearrangement is influenced by water molecules desorption in the early initial stage of densification during sintering of microstructurally inhomogeneous compacts.

Effective activation energies *nQ* of 31 kcal/mol and 32 kcal/mol (where *n* is 1/3 and 1/2 for grain boundary and volume diffusion, respectively) were determined for the NZ25 and NZ20 powder, respectively (Fig. 11). The corresponding activation energies of grain boundary diffusion, *Q*, are thus 93 kcal/mol and 96 kcal/mol. These values correlate well with the value of 92.5 kcal/mol cited by Young and Cutler [3]. In the case of NZ8 powder, the effective activation energy is much lower (10 kcal/mol), which indicates that other mechanisms of densification predominate.

4. Conclusions

Characterization of the properties of morphologically different 3 mol% Y_2O_3-ZrO_2 solid solution nanopowders and corresponding heat treated compacts leads to the following conclusions:

Powder morphology significantly influences the behaviour of powders during a low temperature consolidation process.

The temperature of the biginning of shrinkage depends on the size of the crystallites of the starting powder and their ability to dense and uniform packing within a green product. Smaller crystallites leading to smaller pores reduce the temperature of the biginning of shrinkage.

The temperature of maximum shrinkage and the temperature at which pore closure occurs depend in a similar way.

The closure of the pores at too low temperature and accompanied by trapping gases inside the pores limits final density.

Spectacular pore coarsening at initial stage of sintering occurs in green bodies originated from zirconia hydrothermal nanopowders as a result of desorption of water molecules, rounding pores due to surface diffusion, and particle rearrangement during differential densification. The larger the pores, the higher the temperature needed to cause the process of size reduction and the higher the pore closing temperature. Thus, such a pore coarsening of zirconia nanopowders is disadvantegeos and must be suppressed during manufacturing dense sintered bodies.

The temperature of the beginning of the pore growth and its extent depend on the pore size, which is directly related to the size of the crystallites/grains of the powder and the forming technique used. Reducing the size of the pores reduces the temperature of the beginning of the pore growth and at the same time increases the relative increase in their size during heat treatment.

Acknowledgements

The research was supported by AGH-UST, WIMiC, KCiMO under the statutory work no 11.11.160.617 in 2017.

References

[1] Mayo, M. J., Hague, D. C., Chen, D.-J.: Processing Nanocrystalline Ceramics for Applications in Superplasticity, *Mater. Sci. Eng. A*, A166, (1993), 145–59.
[2] Porter, D. L., Heuer, A. H.: Microstructural development in MgO-partially stabilized zirconia (Mg-PSZ), *J. Am. Ceram. Soc.*, 62, 5-6, (1979), 298–305.
[3] Young, S. W., Cutler, I. B.: Initial Sintering with Constant Rates of Heating, *J. Am. Ceram. Soc.*, 53, 12, (1970), 659–663.
[4] Haberko, K., Pyda, W.:Preparation of Ca-stabilized ZrO2 Micropowders by a Hydrothermal Method, *Advances in Ceramics*, vol. 12, *Science and Technology of Zirconia II*, Claussen. N., Rühle, M., Heuer, A.H. (eds.), The American Ceramic Society, Inc., Columbus, Ohio, (1984), 774–783.
[5] Zych, Ł., Haberko, K.: Filter pressing and sintering of a zirconia nanopowder, *J. Eur. Ceram. Soc.*, 26, (2006), 373–378.
[6] Rühle, M., Heuer, A. H.: Phase Transformations in ZrO_2-containing Ceramics: II, The Martensitic Reaction in t-ZrO_2, Zirconia II, *J. Am. Ceram. Soc.*, 1984.
[7] Suresh, A., Mayo, M. J.: Crystallite and Grain-Size-Dependent Phase Transformations in Yttria-Doped Zirconia, *J. Am. Ceram. Soc.*, 86, (2003), 360-362.
[8] Greskovich, C., Lay, K. W.: Grain Growth in Very Porous Al_2O_3 Compacts, *J. Am. Ceram. Soc.*, 55, 3, (1972), 142–146.
[9] De Jonghe L. C., Rahaman, M. N.: Sintering of Ceramics, in *Handbook of Ceramics, Vol. 1: Materials Science*, Somiya, S. et al. (Eds), Elsevier Academic Press, 2003, Ch. 4, 187–264.
[10] Lach, R., Bućko, M. M., Haberko, K., Sitarz, M., Cholewa-Kowalska, K.: From nanometric zirconia powder to transparent polycrystal, *J. Eur. Ceram. Soc.*, 34, (2014), 4321–4326.
[11] Zhou, Y.-C., Rahaman, M. N., Hydrothermal synthesis and sintering of ultra-fine CeO_2 powders, *J. Eur. Ceram. So*c., 15, (1995), 939-950.
[12] Akash A., Mayo, M. J.: Pore Growth during Initial-Stage Sintering, *J. Am. Ceram. Soc.*, 82, 11, (1999), 2948–52.
[13] Exner, H. E., Müller, C.: Particle rearrangement and Pore Space Coarsening During Solid-State Sintering, *J. Am. Ceram. Soc.,* 92, 7, (2009), 1384-90.

♦

Received 14 August 2017, accepted 23 November 2017.